Finite-Element Methods for Steady-State Population Balance Equations

M. Nicmanis and M. J. Hounslow
Dept. of Chemical Engineering, The University of Cambridge, Cambridge CB2 3RA, U.K.

A finite-element algorithm is developed to solve the population balance equation that governs steady-state behavior of well-mixed particulate systems. Collocation and Galerkin methods are used to solve several test problems in which aggregation, breakage, nucleation and growth (and combinations of these phenomena) occur. It is shown that the Galerkin method must be used in growth problems to obtain a well-conditioned system. In all the cases investigated, density distributions and their moments are accurately predicted by the method. In a direct comparison with the discretized population balance (DPB) of Litster et al. (1995) the finite-element method proves capable of predictions that are typically two orders of magnitude more accurate than those of the DPB. These results were obtained using smaller systems of equations and with considerably less computational power.

Introduction

The population balance equation (PBE) is a statement of continuity for particulate systems. In the case of a continuous mixed-suspension, mixed-product removal (CMSMPR) crystallizer in which aggregation, breakage and growth are occurring the PBE is given by Randolph and Larson (1988) as

$$\frac{n(v)-n_{in}(v)}{\tau}+\frac{d(G(v)n(v))}{dv}=b(v)-d(v) \quad \forall v\in(0,\infty] \tag{1}$$

together with the boundary condition: $n(0)=n_0$. In the above equation $n(v)$ and $n_{in}(v)$ are the number-based density distributions of the product and feed streams with respect to the volume coordinate. $G(v)$ is the volume-dependent growth function and the number density of nuclei present is incorporated into the equation as a boundary condition $n(0)=n_0$. The functions $b(v)$ and $d(v)$ are the birth and death rates of particles of size v due to aggregation and breakage.

In the case of aggregation alone in a CMSMPR crystallizer these rates have been derived by Hulburt and Katz (1964) and are rewritten here as

$$b^a(v)=\int_0^{v/2}\beta(v-w,w)n(v-w)n(w)dw \tag{2}$$

$$d^a(v)=n(v)\int_0^{\infty}\beta(v,w)n(w)dw \tag{3}$$

where the aggregation kernel ($\beta(v,w)$) is a measure of the frequency with which particles of size v and w collide, adhere, and form stable aggregates.

Similar considerations have been used to derived birth and death rates of particles due to breakage. These terms have been derived by Prasher (1987) and are rewritten here as number-based quantities

$$b^b(v)=\int_v^{\infty}\rho(v,w)S(w)n(w)dw \tag{4}$$

$$d^b(v)=S(v)n(v) \tag{5}$$

In the above expressions the breakage function ($\rho(v,w)$) is defined so that the probability that a fragment of a particle originally of size w will be broken into the size interval $(v, v+dv)$ is $\rho\,dv$ and the specific rate of breakage ($S(v)$) is the rate constant for particles of size v.

Hence, in a CMSMPR where aggregation and breakage of particles is occurring simultaneously, the birth and death terms of Eq. 1 are obtained by summation of their components due to aggregation and breakage

Correspondence concerning this article should be addressed to M. J. Hounslow at his current address: Dept. of Chemical and Process Engineering, The University of Sheffield, Sheffield S1 3JD, U.K.
Current address of M. Nicmanis: Unilever Research, Colworth Process. Science Unit, Colworth House, Sharnbrook Bedford MK44 1CQ, UK.

$$b(v) = b^a(v) + b^b(v) \quad (6)$$

$$d(v) = d^a(v) + d^b(v) \quad (7)$$

Design, control and optimization of units in which particulate phenomena occur necessitates solution of the PBE for the density distribution $n(v)$. Along with the number density function, it is often useful to know the moments of $n(v)$ because of their physical significance. The ith moment is defined as

$$m_i = \int_0^\infty v^i n(v) dv \quad (8)$$

m_0 and m_1 represent the total number and total volume of particles in the system. The second moment (m_2) has been shown by Smit et al. (1993) to be useful in predicting the onset of gelation.

The combination of differential, integral, and nonlinear terms in the PBE (1) result in an equation for which very few analytical solutions have been found. Hence, those modeling particulate systems frequently resort to numerical methods. These methods usually fall into two broad categories: (a) finite-element methods (FEMs)/methods of weighted residuals (MWRs) in which the solution is approximated as linear combinations of basis functions over a finite number of subdomains (termed "elements"), and (b) finite difference methods (FDMs)/discretized population balances (DPBs) in which Eq. 1 is approximated by difference schemes.

Of the finite-element schemes, the earliest reported is that of Gelbard and Seinfeld (1978). Their application incorporated piecewise C^1 and C^2 cubic polynomials into a collocation formulation to solve the dynamic PBE with aggregation and growth terms. The domain of the independent variable was scaled logarithmically and then spanned by elements of equal sizes, possibly to avoid problems with ill-conditioned systems that will be discussed later in this article. The finite-element method was later applied to the same problem by Eyre et al. (1988) and Viljoen et al. (1990). These applications used cubic B-splines as basis functions in a collocation formulation but scaled the domain with a singular function. This method did not consider breakage terms.

The main alternative to finite-element methods has been DPBs. These methods are essentially differencing schemes over domains that are usually partitioned according to a geometric progression. Birth and death terms are deduced by considering all possible mechanisms by which particles can move from one partition to another. Schemes of this nature have been proposed to solve the aggregation and growth PBE by Batterham et al. (1981), Marchal et al. (1988), Hounslow et al. (1988), and Litster et al. (1995), while Hill and Ng (1995) have proposed a DPB to solve the breakage problem. Later in this article, it will be shown that these methods are computationally inefficient compared to finite-element methods.

Comprehensive reviews of DPB, FEM, and several alternative methods for solving the PBE have been compiled by Ramkrishna (1985).

Formulation of the Finite-Element Algorithm

Use of an unscaled domain

In some cases domain scaling may make the prediction of large numbers of small particles easier. However, it usually makes the task of predicting small numbers of large particles much more difficult. Small errors in the density distribution at the larger size ranges are multiplied by exponential factors when the solution is transformed back to its original coordinates. It is also much more difficult to calculate the moments of the density distribution over a scaled domain. For instance, calculation of the second moment over a domain scaled with the singular function used by Eyre et al. (1988) would require integration of a function that had been reduced to a spike in the transformed domain.

Another problem inherent in the previously mentioned finite-element methods is that they are reliant upon well-chosen mapping parameters. Eyre et al. (1988) acknowledge that a good choice of their mapping parameter (ζ) is critical for the success of their method but make no suggestion apart from trial and error as to how to select this value.

The above mentioned problems will here be avoided by deriving the algorithm over an unscaled domain and solving the resulting system of equations over elements with lengths that increase with increasing volume.

Truncation of the infinite domain

The infinite domain of expression 1 must be truncated to a finite upper limit, so that it may be spanned by a finite number of elements. This truncation results in an underestimation of the integrals of expressions 3 and 4 which reduce Eq. 1 to an approximation of the PBE over a finite domain. It can also be anticipated that the ith moment of the solution will be underestimated by an amount

$$m_i^{dte} = \int_{v_{\max}}^\infty v^i n(v) dv \quad (9)$$

where m_i^{dte} is the error incurred in the ith moment due to domain truncation and $v_{\max}$ is the upper limit of the finite domain. In most practical applications the density distribution ($n(v)$) asymptotes towards zero at sufficiently large particle volumes, so $v_{\max}$ can be selected to be sufficiently large that such underestimation is negligibly small.

Care must be taken to avoid selection of unnecessarily large values of $v_{\max}$ since tail regions can be difficult and/or computationally expensive to converge, because of the very small values they can attain at large particle volumes.

Little attention has been paid to systematic methods of selecting appropriate upper limits of the domain. Gelbard and Seinfeld (1978) define quantities M_i

$$M_i = \frac{\int_0^{v_{\max}} v^i n(v) dv}{m_i} \quad (10)$$

and select $v_{\max}$ such that M_0 and M_1 do not differ appreciably from unity. This approach is limited to cases where an analytical expression for m_i is available.

In Appendix A a systematic method will be suggested for selection of values of $v_{\max}$ that will approximately satisfy the criterion

$$M_2 > 0.999 \quad (11)$$

If $M_2 > 0.999$ then the additional criteria $M_0 > 0.999$ and $M_1 > 0.999$ will also be satisfied. Another motivation for using a

criterion based on M_2 (as opposed to M_0 or M_1) is the authors' interest in predicting the onset of gelation.

Partitioning of the domain

The truncated domain $\Omega = (0, v_{max})$ is partitioned into N discrete elements: $\Omega_e = (v_a^e, v_b^e)$, $e = 1, 2, \ldots, N$ such that: $\cup_{e=1}^{N} \Omega_e = \Omega$ and $\cap_{e=1}^{N} \Omega_e = \emptyset$.

In this article the upper limits of the subdomains are positioned according to the geometrical progression

$$v_b^e = v_b^1 \left(\frac{v_{max}}{v_b^1} \right)^{\frac{e-1}{N-1}} \tag{12}$$

where superscripts 1 and e denote the first and eth elements, v_b^e denotes the upper limit of element e, and N is the total number of elements used to span the domain. The resulting partition is finer for small volumes (where the solution is changing rapidly) and coarser at large volumes (where the solution is changing comparatively slowly).

Refinement of the Partition. Once the upper limit of the domain (v_{max}) is established, two adjustable parameters define the above-mentioned geometrical progression: (i) the length of the first element and (ii) the number of elements in the partition. The values of these parameters are selected using the following procedure:

(1) The domain is truncated, partitioned and the problem is solved for the density distribution and its moments (using the finite-element method described in the next section).

(2) The length of the first element is reduced and the problem re-solved until further reductions result in insignificant changes in the zeroth moment.

(3) The number of elements is increased and the problem re-solved until further increases in numbers of elements make insignificant changes to the value of the 2nd moment.

Unlike the DPBs, the finite-element method to be described in the next section makes no assumptions that dictate node placement schemes. Hence, the FEM is amenable to more sophisticated methods of node placement and mesh refinement. These methods are based upon an error estimate, the derivation of which is beyond the scope of this article. Further details of the error estimate and adaptive mesh refinement algorithms are given in Nicmanis and Hounslow (1998a,b).

Approximation of solution

Consider the eth element $\Omega^e = (v_a^e, v_b^e]$. Within this element, the solution to Eq. 1 will be approximated as a polynomial of order $p-1$. This polynomial will take the form of a linear combination of Lagrange polynomials, the p zeros of which will be termed the nodes of the element. In this article the first and last node of element e will correspond to v_a^e and v_b^e, respectively, with the rest of the nodes equally spaced within the element

$$n(v) \approx n_h^e(v) = \sum_{j=1}^{p} n_j^e \psi_j^e(v) \quad \forall v \epsilon (v_a^e, v_b^e) \tag{13}$$

where the n_js are the nodal values of the density distribution, the $\psi_j(v)$s are the standard Lagrange interpolation polynomials of order $p-1$.

Formation of weighted residual expressions

Equation 1 is then rearranged to obtain the following form

$$n(v) r[v,n] + \tau G(v) \frac{dn(v)}{dv} = n_{in}(v) + \tau b[v,n] \tag{14}$$

where

$$r[v,n] = \left[1 + \tau \left(\bar{d}[v,n] + \frac{dG(v)}{dv} \right) \right] \tag{15}$$

The arguments of the birth and death terms are used to indicate that they have functional dependencies on the unknown density distribution $n(v)$. A modified death term has also been introduced to simplify notation

$$\bar{d}[v,n] = \frac{d^a(v) + d^b(v)}{n(v)} \tag{16}$$

and the birth term is assumed to contain components due to both aggregation and breakage as in Eq. 6.

A weighted residual statement is formed from expression 14 by multiplying by a weight function $\phi(v)$ and integrating over the domain of the element

$$\int_{v_a^e}^{v_b^e} \phi(v) \left\{ n(v) r[v,n] + \tau G(v) \frac{dn(v)}{dv} \right\} dv = \int_{v_a^e}^{v_b^e} \phi(v) \{ n_{in}(v) + \tau b[v,n] \} dv \tag{17}$$

Substitution of $n(v)$ by $n_h^e(v)$ yields

$$\sum_{j=1}^{p} \int_{v_a^e}^{v_b^e} \phi(v) \left\{ \psi_j^e(v) r[v,n] + \tau G(v) \frac{d\psi_j^e(v)}{dv} \right\} dv \cdot n_j^e = \int_{v_a^e}^{v_b^e} \phi(v) \{ n_{in}(v) + \tau b[v,n] \} dv \tag{18}$$

Equation 18 is used to generate a set of p equations by substitution of the set of p weight functions $\{\phi_i^e(v)\}_{i=1}^{p}$ for $\phi(v)$

$$\sum_{i=j}^{p} \int_{v_a^e}^{v_b^e} \phi_i^e(v) \left\{ \psi_j^e(v) r[v,n] + \tau G(v) \frac{d\psi_j^e(v)}{dv} \right\} dv \cdot n_j^e = \int_{v_a^e}^{v_b^e} \phi_i^e(v) \{ n_{in}(v) + \tau b[v,n] \} dv \tag{19}$$

where $i = 1, 2, \ldots, p$. Or, in matrix notation

$$A^e n^e = F^e \tag{20}$$

where

$$A^e_{ij} = \int_{v_a^e}^{v_b^e} \phi_i^e(v) \left\{ \psi_j^e(v) r[v,n] + \tau G(v) \frac{d\psi_j^e(v)}{dv} \right\} dv \tag{21}$$

and

$$F_i^e = \int_{v_a^e}^{v_b^e} \phi_i^e(v) \{ n_{\text{in}}(v) + \tau b[v,n] \} dv \tag{22}$$

Collocation Formulation. In the collocation formulation the weight functions are taken to be a set of Dirac delta functions

$$\phi_i^e(v) = \delta(v - v_i^e) \quad \forall i = 1, 2, \ldots, p \tag{23}$$

where the v_i^es are the collocation points and are selected such that $v_i^e \in (v_a^e, v_b^e] \quad \forall i = 1, 2, \ldots, p$. With this set of weight functions, expressions 21 and 22 become

$$A^e_{ij} = \int_{v_a^e}^{v_b^e} \delta(v - v_i^e) \left\{ \psi_j^e(v) r[v,n] + \tau G(v) \frac{d\psi_j^e(v)}{dv} \right\} dv \tag{24}$$

and

$$F_i^e = \int_{v_a^e}^{v_b^e} \delta(v - v_i^e) \{ n_{\text{in}}(v) + \tau b[v,n] \} dv \tag{25}$$

Further simplification can be made using the definition of the Dirac delta

$$A^e_{ij} = \psi_j^e(v_i^e) r[v_i^e, n(v_i^e)] + \tau G(v_i^e) \frac{d\psi_j^e(v_i^e)}{dv} \tag{26}$$

$$F_i^e = n_{\text{in}}(v_i^e) + \tau b[v_i^e, n(v_i^e)] \tag{27}$$

Hence, in the collocation formulation the PBE is enforced by means of pointwise evaluations within each element.

Galerkin Formulation. In the Galerkin formulation the interpolation functions are also used for the weight functions

$$\phi_i^e(v) = \psi_i^e(v) \quad \forall i = 1, 2, \ldots, p \tag{28}$$

The expressions 21 and 22 then become

$$A^e_{ij} = \int_{v_a^e}^{v_b^e} \psi_i^e(v) \left\{ \psi_j^e(v) r[v,n] + \tau G(v) \frac{d\psi_j^e(v)}{dv} \right\} dv \tag{29}$$

and

$$F_i^e = \int_{v_a^e}^{v_b^e} \psi_i^e(v) \{ n_{\text{in}}(v) + \tau b[v,n] \} dv \tag{30}$$

Hence, the Galerkin formulation enforces the PBE by means of integral averages over each element.

Nodal approximation of birth and death terms

At this stage of the derivation, the birth terms for aggregation ($b^a[v,n]$ and $b^b[v,n]$) and the death term for aggregation ($d^a[v,n]$) are still operators on the unknown density distribution ($n(v)$). These expressions must be reformulated in terms of their nodal values before Eq. 20 can be solved. In this subsection (and for the remainder of this article) it will be assumed that nodes are spaced evenly within each element and that Lagrange cubics have been used for the interpolation functions. Under these two assumptions, a Newton-Cotes fixed point rule can be use to perform the integrations. Generalization to polynomials of any order and nonevenly spaced nodes can be made with the combination of an appropriate integration rule and a transformation to an element with evenly spaced nodes.

Approximation of the Death Term for Aggregation. Calculation of $r[v,n]$ of expression 15 requires an approximation of the following modified death term for aggregation

$$\bar{d}^a[v,n] = \frac{d^a[v,n]}{n(v)} = \int_0^\infty \beta(v,w) n(w) dw \tag{31}$$

The integrand of expression 31 is evaluated at the four nodal coordinates $(v_1^e, v_2^e, v_3^e, v_4^e)$ of each element. Integration is then performed over each element using a Newton-Cotes 3/8 rule weighting of these functional evaluations. The modified death term for aggregation results from the sum of these integrations.

$$\bar{d}^a[v,n] \approx \sum_{e=1}^{N} \left(\frac{v_4^e - v_1^e}{3} \left[\frac{3}{8} \beta(v, v_1^e) n_1^e + \frac{9}{8} \beta(v, v_2^e) n_2^e + \frac{9}{8} \beta(v, v_3^e) n_3^e + \frac{3}{8} \beta(v, v_4^e) n_4^e \right] \right) \tag{32}$$

In the above approximation N is the number of elements, v_i^e is the volume coordinate of the ith node of element e and n_i^e is the ith nodal value of the number density distribution of element e.

Approximation of Birth Term for Aggregation. To calculate the birth term for aggregation ($b^a[v,n]$ in Eq. 2), let $v/2$ lie in element e. The first $e-1$ terms are evaluated as for the death term by making functional evaluations of the integrand of $b^a(v)$ at the nodes of the appropriate elements and applying a Newton-Cotes rule weighting to perform an integration over each element. Hence, the contribution from the kth ($k = 1, 2, \ldots, e-1$) element is

$$b_k^a(v) = \frac{v_4^k - v_1^k}{3} \left[\frac{3}{8} \beta(v - v_1^k, v_1^k) \bar{n}(v - v_1^k) n_1^k + \frac{9}{8} \beta(v - \tfrac{k}{2}, v_2^k) \bar{n}(v - v_2^k) n_2^k + \frac{9}{8} \beta(v - v_3^k, v_3^k) \bar{n}(v - v_3^k) n_3^k + \frac{3}{8} \beta(v - v_4^k, v_4^k) \bar{n}(v - v_4^k) n_4^k \right] \tag{33}$$

In the above expression $\bar{n}(v^*)$ is the cubic polynomial passing through the four points $(v_i^l, n_i^l)_{i=1}^4$ evaluated at v^* where $v^* \in (v_1^l, v_4^l]$. Note that when evaluating $b_k(v)$, v^* does not necessarily lie in element k.

The contribution from the eth element is

$$b_e^a(v) = h\left[\frac{3}{8}\beta(v - v_1^e, v_1^e)\bar{n}(v - v_1^e)\bar{n}(v_1^e) + \frac{9}{8}\beta(v - \bar{v}_2^e, \bar{v}_2^e)\bar{n}(v - \bar{v}_2^e)\bar{n}(\bar{v}_2^e) + \frac{9}{8}\beta(v - \bar{v}_3^e, \bar{v}_3^e)\bar{n}(v - \bar{v}_3^e)\bar{n}(\bar{v}_3^e) + \frac{3}{8}\beta\left(\frac{v}{2}, \frac{v}{2}\right)\left\{\bar{n}\left(\frac{v}{2}\right)\right\}^2\right] \quad (34)$$

where $h = (v/2 - v_1^e)/3$, $v_2^e = v_1^e + h$ and $v_3^e = v_1^e + 2h$. These contributions are summed to obtain the following approximation of the birth term for aggregation

$$b^a(v) \approx \sum_{k=1}^{e-1} b_k^a(v) + b_e^a(v) \quad (35)$$

Approximation of Birth Term for Breakage. Let v lie in element e, that is, $v \in (v_a^e, v_b^e]$. Then, the contribution from the eth element to the birth term for breakage ($b^b[v, n]$ in Eq. 4) is

$$b_e^b(v) = h\left[\frac{3}{8}\rho(v, v)S(v)\bar{n}(v) + \frac{9}{8}\rho(v, \bar{v}_1^e)S(\bar{v}_1^e)\bar{n}(\bar{v}_1^e) + \frac{9}{8}\rho(v, \bar{v}_2^e)S(\bar{v}_2^e)\bar{n}(\bar{v}_2^e) + \frac{3}{8}\rho(v, v_4^e)n_4^e\right] \quad (36)$$

where $h = (v_4^e - v)/3$, v_i^e is the ith node of element e, $\bar{v}_1^e = v + h$, $\bar{v}_2^e = \bar{v}_1^e + h$, n_i^e is the ith nodal value of element e, and $n(v)$ is the cubic passing through the four points $(v_i^e, n_i^e)_{i=1}^4$. The contribution from the kth ($k = e+1, \ldots, N$) element is

$$b_k^b(v) = \frac{v_4^k - v_1^k}{3}\left[\frac{3}{8}\rho(v, v_1^k)S(v_1^k)n_1^k + \frac{9}{8}\rho(v, v_2^k)S(v_2^k)n_2^k + \frac{9}{8}\rho(v, v_3^k)S(v_3^k)n_3^k + \frac{3}{8}\rho(v, v_4^k)S(v_4^k)n_4^k\right] \quad (37)$$

These contributions are summed to give the following approximation of the birth term for breakage

$$b^b(v) \approx b_e^b(v) + \sum_{k=e+1}^{N} b_k^b(v) \quad (38)$$

Assembly of elements into global system

Equation 20 results in a system of p equations for each of the N elements of the domain, or a total of $N \times p$ equations. This number is reduced to $N \times (p-1) + 1$ (which is the number of unknown nodal values (n_is) of the global system) by imposing continuity at the end points of the elements. The standard procedure of assembling the elemental matrices is performed as described by Zienkiewicz and Taylor (1989), resulting in a global system of equations. The global matrix consists of a diagonal of N, $p \times p$ blocks

$$A_{ij}^g[\boldsymbol{n}]n_j = F_i^g[\boldsymbol{n}] \quad (39)$$

where $i, j = 1, \ldots, N \times (p-1) + 1$. The superscript g indicates elements of a global matrix or vector and arguments have been included to indicate that these elements are dependent upon the unknown nodal values of the density distribution.

Aggregation and Breakage Problems. In cases where aggregation and/or breakage (but no growth, that is, $G(v) = 0$) occur, the boundary condition is not required. If both sides of the above equation are divided by $r[v, n]$, then the global matrix becomes independent of the vector of unknown nodal values (which reduces the computational expense of solving the global system since the A-matrix must only be decomposed once)

$$A_{ij}^g n_j = F_i^g[n_j] \quad (40)$$

where the elemental contributions are

$$A_{ij}^e = \phi_j^e(v_i^e) \quad (41)$$

$$F_i^e = \frac{n_{\text{in}}(v_i^e) + \tau b[v_i^e, n]}{r[v_i^e, n]} \quad (42)$$

for the collocation formulation, or

$$A_{ij}^e = \int_{v_a^e}^{v_b^e} \phi_i^e(v)\phi_j^e(v)dv \quad (43)$$

$$F_i^e = \int_{v_a^e}^{v_b^e} \phi_i^e(v)\frac{n_{\text{in}}(v) + \tau b[v, n]}{r[v, n]}dv \quad (44)$$

for the Galerkin formulation.

Growth Problems. In all cases where particle growth is occurring the boundary condition must be enforced at $v = 0$ for a unique solution to exist. Hence, the number of equations and unknowns is reduced to the following system of $N \times (p-1)$ equations

$$A_{ij}^g[\boldsymbol{n}]n_j = F_i^g[\boldsymbol{n}] - A_{i1}^g[\boldsymbol{n}]n_0 \quad (45)$$

where $i, j = 2, \ldots, N \times (p-1) + 1$. It is possible to rearrange the above equation so that the A matrix becomes independent of the vector of unknown density distributions. However, this has been avoided since the resulting system of equations can be difficult to converge.

Solution of the global system of equations

The systems of Eqs. 40 and 45 are nonlinear; hence, iterative schemes are used to solve them. In aggregation and

breakage problems the $s+1$th estimate of the vector of nodal values is determined from the sth estimate by solving the system

$$A^g_{ij} n_j^{s+1} = F_i^g[\boldsymbol{n}^s] \tag{46}$$

The A^g matrix is decomposed using subroutines described by Press et al. (1992) for banded linear systems. Since this matrix is independent of the nodal values, decomposition need only be performed once. A new improved estimate of the unknown nodal values is obtained by using the back-substitution algorithms (also described by Press et al.) on the F^g vector which is calculated using the nodal values from the previous iteration.

In growth problems the $s+1$th estimate of the vector of nodal values is determined from the sth estimate by solving the system

$$A^g_{ij}[\boldsymbol{n}^s] n_j^{s+1} = F_i^g[\boldsymbol{n}^s] - A^g_{i1}[\boldsymbol{n}^s] n_0 \tag{47}$$

In this case both the A^g matrix and the F^g vector must be determined using the nodal values from the previous iteration. Decomposition and back-substitution are both performed in each iteration.

In all the case studies discussed in the next section the iterative procedure is initialized using the feed distribution. Iterations are continued until the change in each of the nodal values is less than 0.01% of that in the previous iteration.

Attempts were made to solve the systems of Eqs. 46 and 47 using the Newton-Raphson methods described by Press et al., but these methods proved to be difficult, and in many cases expensive, to converge. The latter factor was due to the requirement of this method to assemble and decompose a completely dense $N \times N$ Jacobian matrix.

Numerical case studies

The finite-element method was applied to four cases of the PBE for which analytical solutions are known. Aggregation, breakage, and growth were each studied as isolated phenomena in the first three cases while aggregation, growth, and nucleation were investigated in the final case. The ability of the method to correctly predict the number of particles in an interval was compared to that of the DPB of Litster et al. (1995) in the aggregation problem.

Case 1: Aggregation. The PBE for aggregation alone is obtained by setting the breakage function, the specific rate of breakage, and the growth function to zero

$$\rho(v,w) = 0 \quad \forall v,w \tag{48}$$

$$S(v) = 0 \quad \forall v \tag{49}$$

$$G(v) = 0 \quad \forall v \tag{50}$$

For the idealized case of an exponential feed distribution

$$n_{\text{in}}(v) = \frac{N_0}{v_0} \exp\left(\frac{-v}{v_0}\right) \tag{51}$$

and a size-independent aggregation kernel

$$\beta(v,w) = \beta_0 \tag{52}$$

the analytical solution has been derived by Hounslow (1990) as

$$n(v) = \frac{N_0}{v_0} \frac{I_0\left[\dfrac{-tv}{v_0(1+2t)}\right] + I_1\left[\dfrac{-tv}{v_0(1+2t)}\right]}{\sqrt{1+2t}\,\exp\left[\dfrac{(1+t)v}{(1+2t)v_0}\right]} \tag{53}$$

where I_0 and I_1 are modified Bessel functions of the first kind of zeroth and first orders and $t = \beta_0 N_0 \tau$. An asymptotic expansion of the above solution has been derived by Hounslow (1998) for $v \to \infty$

$$n(v) = \frac{\exp\left[\dfrac{-v}{2v_0 t}\right]}{\sqrt{\pi}\,(2t)^2\left[\dfrac{v}{2v_0 t}\right]^{3/2}} \tag{54}$$

and is used when

$$\frac{tv}{v_0(1+2t)} > 700 \tag{55}$$

since the values of the modified Bessel functions exceed the numerical range of most processors for such arguments.

The constants N_0, v_0, and β_0 were set to unity and three different problems were defined by specifying three different time constants (τ values) which are listed in Table 1.

Analytical expressions for the zeroth, first and second moments of the solution (m_0, m_1 and m_2) have been derived by Smit et al. (1993) to be

$$m_0 = \frac{-1 + \sqrt{1 + 2\beta_0 m_0^{\text{in}} \tau}}{\beta_0 \tau} \tag{56}$$

$$m_1 = m_1^{\text{in}} \tag{57}$$

$$m_2 = \beta_0 m_1^2 \tau + m_2^{\text{in}} \tag{58}$$

The above expressions have been used to evaluate the moments for each of the simulations performed. These values are tabulated in Table 1. Also tabulated is the index of aggregation (I_{agg}) which has been defined by Hounslow (1990)

$$I_{agg} = 1 - \frac{m_0}{m_0^{\text{in}}} \tag{59}$$

Table 1. Analytical Moments of Density Distribution and Indices of Aggregation

Case	τ	m_0	m_1	m_2	I_{agg}
1a	2×10^2	9.51×10^{-2}	1	202	0.9049
1b	2×10^4	9.95×10^{-3}	1	20,002	0.9901
1c	2×10^6	9.99×10^{-4}	1	200,002	0.9990

Table 2. Domain Truncation and Partition Parameters Used in the Aggregation Problem

Case	v_{max}^0	M_2^0	v_{max}	M_2	v_1	N
1a	2.500×10^{3}	0.9940	3.306×10^{3}	0.9990	1.0	32
1b	2.500×10^{5}	0.9941	3.294×10^{5}	0.9990	1.5	40
1c	2.500×10^{7}	0.9941	3.403×10^{7}	0.9993	2.0	45

and is used as a quantitative measure of the extent to which complete aggregation has been achieved. This index can attain values between zero (no aggregation) and one (complete aggregation).

Truncation and mesh refinement were performed as previously described. An initial estimate of the truncation point (v_{max}^0) was located by visual inspection. The extrapolation procedure for aggregation/growth dominant problems was then used to obtain an improved estimate of a truncation point (v_{max}) satisfying criterion 11. These estimates are recorded in Table 2. Also tabulated are the quantities M_2^0 (M_2 of Eq. 10 using v_{max}^0 as an upper limit) and M_2 (which uses v_{max} as an upper limit). These quantities were evaluated using the analytical expressions 53 and 54 as a check on the appropriateness of the truncation points. In the final two columns of Table 2 the length of the first element and the number of elements used to span the truncated domain are recorded. These are the parameters of the geometrical progression used in the final refined partition to generate the results listed in Table 3.

The collocation formulation of the aggregation problem was solved using the successive substitution strategy (Eq. 46). The finite-element predictions of the number density function ($n(v)$) are shown in Figure 1. Large relative errors are most likely to be present in the tail region of the density distribution. For this reason, the results are plotted on log-log axes. The solid lines represent the analytical solution while the symbols are the nodal values of the finite-element solution for the first and last node of each element.

A mean-square relative error in the number of particles predicted in an interval can be defined as a measure of the quality of a solution

$$\frac{1}{N}\,\mathrm{SSRE} = \frac{1}{N}\sum_{i=1}^{N}\left(\frac{m(i)_0^{fea} - m(i)_0^{ana}}{m(i)_0^{ana}}\right)^2 \qquad (60)$$

In the above expression $m(i)_0$ is the number of particles in the ith partition and the superscripts *fea* and *ana* denote predictions of the finite-element solution and the analytical solution respectively. Values of $1/N$ SSRE and the percentage error of the moments of the finite-element solution

Table 3. Errors in Moments and Mean Square Relative Errors of the Finite-Element Solution to the Aggregation Problem

Case	Em_0	Em_1	Em_2	$1/N$ SSRE	N_{eq}	CPU	N_{it}
1a	0.003%	0.023%	0.134%	2.008×10^{-9}	97	$4u$	257
1b	0.016%	0.073%	0.192%	7.256×10^{-8}	121	$64u$	2,121
1c	0.051%	0.095%	0.139%	6.325×10^{-7}	136	$573u$	16,377

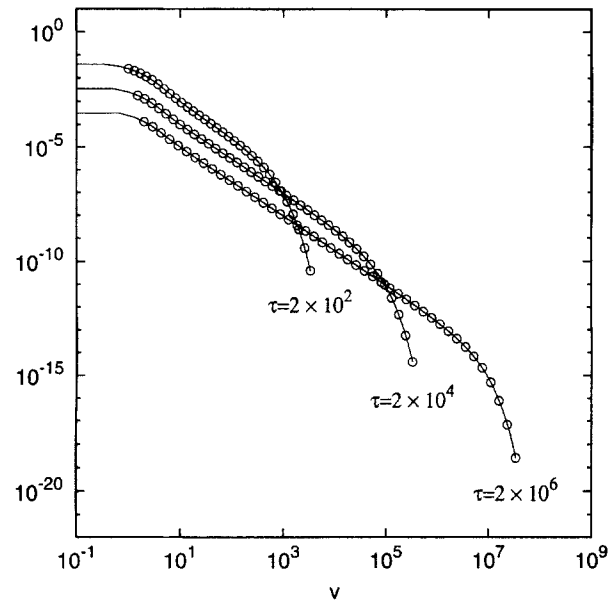

Figure 1. FEM predictions of number density function $n(v)$ for aggregation problem.

(Em_i) are recorded in Table 3. Also tabulated was the number of equations comprising the system (N_{eq}), the number of iterations required for the system to converge (N_{it}) and CPU requirements of the Sun Ultra Enterprise II that were used to solve the system (CPU). One CPU unit corresponds approximately to one second of real time.

The simulations were repeated using the DPB of Litster et al. (1995) as modified by Wynn (1996). Prior to implementing this method, the domain must be truncated to a nonzero lower limit ($0 < v_{min}$) as well as a finite upper limit ($v_{max} < \infty$). Hence, domain truncation errors are incurred at both the lower and upper limits of the domain. The lower limit was selected to be as large as possible such that the criterion

$$\frac{\int_{v_{min}}^{\infty} n(v)dv}{\int_{0}^{\infty} n(v)dv} > 0.999 \qquad (61)$$

was still satisfied.

In an attempt to match the accuracy of the finite-element method, increasingly large discretization factors (q values) were used. Once the discretization factor was set, the number of equations used to approximate the system (N_{eq}) was selected to be as small as possible such that $M_2 > 0.999$. This in turn dictated the upper limit of the domain (v_{max}). When a discretization factor of $q = 24$ was reached, the resulting systems of equations became too large to solve with the existing computer resources. The parameters of the DPB simulations with a discretization factor of $q = 23$ are listed in Table 4.

Figure 2 is a plot of the square relative error in the number of particles predicted in an interval by the DPB and the finite-element method in case 1b. The square relative errors for the DPB appear as boxes while those of the finite-element method appear as crosses. Errors in moments of the DPB solution, mean-square relative errors, number of equations comprising the system, and CPU times are recorded in Table 5.

Table 4. Domain Truncation and Partition Parameters Used for DPB When Solving the Aggregation Problem

Case	τ	v_{min}	v_{max}	N_{eq}
DPBa	2×10^{2}	0.001	3.526×10^{3}	502
DPBb	2×10^{4}	0.001	3.421×10^{5}	653
DPBc	2×10^{6}	0.002	3.646×10^{7}	781

Case 2: Breakage. To obtain the PBE for breakage the aggregation kernel and the growth function were both set to zero

$$\beta(v,w)=0 \quad \forall v,w \tag{62}$$

$$G(v)=0 \quad \forall v \tag{63}$$

As in the aggregation problem, the exponential feed distribution was used. For the breakage problem with a binary breakage function and size-dependent rate of breakage

$$\rho(v,w)=\frac{2}{w} \tag{64}$$

$$S(v)=v \tag{65}$$

the solution is derived in Appendix B as

$$n(v)=\frac{N_0\left[(1+\tau v)^2+2\tau v_0(1+\tau[v_0+v])\right]}{v_0(1+\tau v)^3\exp\left(\frac{v}{v_0}\right)} \tag{66}$$

An alternative derivation has been given by McGrady and Ziff (1988).

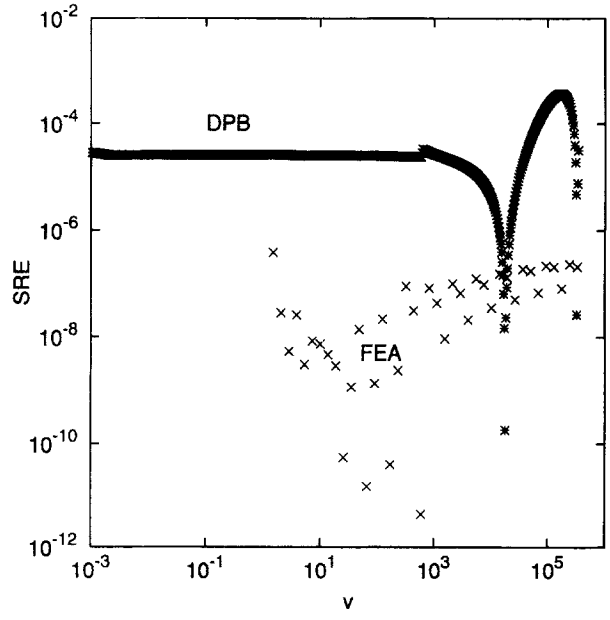

Figure 2. Square relative errors for the finite-element algorithm and DPB of Litster et al. (1995) in case 1b.

Table 5. Errors in Moments and Mean Square Relative Errors of the DPB Solution to Aggregation Problem

Case	Em_0	Em_1	Em_2	$1/N$ SSRE	N_{eq}	CPU
DPBa	0.052%	0.000%	0.194%	2.591×10^{-4}	501	$216u$
DPBb	0.451%	0.000%	0.753%	4.034×10^{-5}	653	$469u$
DPBc	0.052%	0.000%	0.163%	7.101×10^{-5}	781	$731u$

The constants N_0 and v_0 were set to unity and the breakage problem was solved for the three time constants listed in Table 6.

An analytical expression for the zeroth moment can be derived by integrating the PBE for breakage over the volume domain $v \in (0,\infty)$

$$m_0=\tau m_1+m_0^{in} \tag{67}$$

It is assumed that total particle volume is conserved for pure breakage systems; hence, the first moment of the feed distribution will be the same as that of the product stream

$$m_1^{in}=m_1 \tag{68}$$

The above analytical expressions were used to calculate the zeroth and first moments for each of the time constants listed in Table 6. An analytical expression of the second moment can only be derived in terms of the third moment (which can only be derived in terms of the fourth moment and so forth), hence, semi-analytical values of the second moment were obtained by numerical integration of the function $v^2n(v)$ where $n(v)$ is the solution to the breakage PBE (66). An index of breakage I_{bre} can be defined by analogy with the index of aggregation

$$I_{bre}=1-\frac{m_0^{in}}{m_0} \tag{69}$$

Analytical and semi-analytical evaluation of the moments of the solution and indices of breakage are recorded in Table 6.

Domain truncation was performed using the method described previously for breakage dominant problems. Truncation points (initial and final estimates), corresponding M_2 values and the parameters of the refined geometrical progression are recorded in Table 7.

As in the previous case, the successive substitution scheme (Eq. 46) was used to solve the collocation formulation of the problem. A log-log plot of the finite-element predictions of the number density function ($n(v)$) is shown in Figure 3. The solid lines represent the analytical solution while the symbols

Table 6. Analytical Moments of Density Distribution and Indices of Breakage

Case	τ	m_0	m_1	m_2	I_{bre}
2a	1×10^{0}	2	1	1.192×10^{0}	0.5000
2b	1×10^{2}	101	1	8.157×10^{-2}	0.9901
2c	1×10^{4}	10,001	1	1.727×10^{-3}	0.9999

Table 7. Domain Truncation and Partition Parameters Used in Breakage Problem

Case	v_{max}^0	M_2^0	v_{max_1}	v_{max_2}	M_2	v_1	N
2a	12	1.0000	9.2373	15.629	0.9991	1×10^{-1}	15
2b	12	1.0000	7.4129	13.668	0.9992	1×10^{-3}	30
2c	12	1.0000	6.7777	12.981	0.9993	1×10^{-5}	50

are the nodal values of the finite-element solution for the first and last node of each element. It should be noted that the solutions are only plotted in the interval $(0, v_{max_1})$ since the solution over the interval (v_{max_1}, v_{max_2}) contains significant truncation errors and was only computed in order to reduce the truncation error in the birth rate due to breakage within the interval $(0, v_{max_1})$. Moments of the finite-element solution were calculated and the errors in these moments along with the $1/N$ SSRE values, number of equations to be solved, CPU requirements to solve the equations, and the number of iterations required for convergence are recorded in Table 8.

Case 3: Growth. The PBE for growth alone was obtained by setting the aggregation kernel, the breakage function and the specific rate of breakage to zero

$$\beta(v,w) = 0 \quad \forall v,w \tag{70}$$

$$\rho(v,w) = 0 \quad \forall v,w \tag{71}$$

$$S(v) = 0 \quad \forall v \tag{72}$$

The normalized feed distribution

$$n_{in}(v) = \frac{N_0 v}{v_0^2} \exp\left(-\frac{v}{v_0}\right) \tag{73}$$

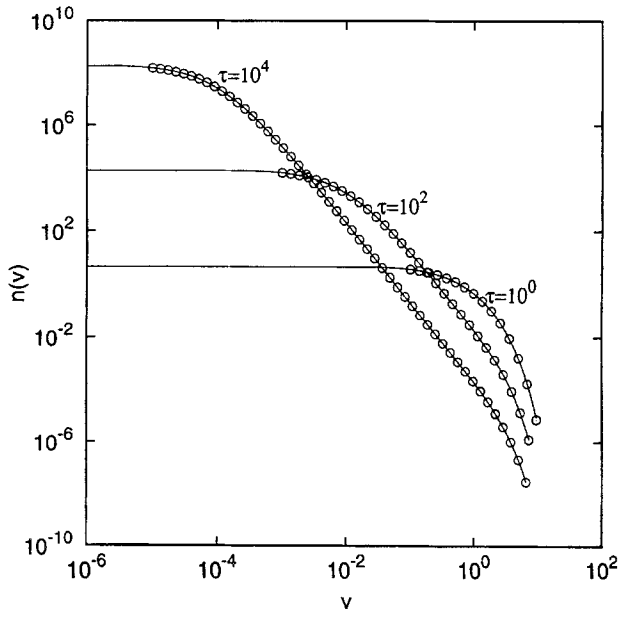

Figure 3. FEM predictions of the number density function ($n(v)$) for the breakage problem.

Table 8. Errors in Moments and Mean Square Relative Errors of the Finite-Element Solution to Breakage Problem

Case	Em_0	Em_1	Em_2	$1/N$ SSRE	N	CPU	N_{it}
2a	0.003%	0.047%	0.142%	1.105×10^{-5}	15	$<1u$	15
2b	0.192%	0.189%	0.278%	1.160×10^{-4}	30	$<1u$	36
2c	0.270%	0.267%	0.308%	2.054×10^{-4}	50	$298u$	79

was used in this series of problems. Since the resulting PBE contains a derivative term, the boundary condition $n(0)$ must be specified in order to obtain a unique solution. This condition was set to zero

$$n(0) = 0 \tag{74}$$

This combination of feed distribution and boundary condition was used to obtain a pure growth problem (without nucleation) with a continuous solution. A constant growth function was selected for this problem

$$G(v) = G_0 \tag{75}$$

Although not physically realistic, a constant growth rate results in a PBE for which the solution may be trivially derived as

$$n(v) = \frac{N_0(vv_0 - \tau G_0[v - v_0])}{v(\tau G_0 - v_0)^2 \exp(v/v_0)} \tag{76}$$

It should be noted that this solution becomes singular when $v_0 = \tau G_0$. In this special case an alternate analytical solution may be derived

$$n(v) = \frac{N_0(2v + \tau G_0)}{4(\tau G_0)^2 \exp(v/(\tau G_0))} \quad \text{if} \quad v_0 = \tau G_0 \tag{77}$$

Simulations were performed with N_0 and v_0 set to unity for each of the three τG_0 values listed in Table 9.

Analytical expressions for the zeroth, first, and second moment may be obtained by multiplying the PBE for breakage by v^i (where i is the appropriate index) and integrating over the volume domain. This procedure results in the following three expressions

$$m_0 = m_0^{in} \tag{78}$$

$$m_1 = m_1^{in} + \tau G_0 m_0 \tag{79}$$

$$m_2 = m_2^{in} + 2\tau G_0 m_1 \tag{80}$$

Table 9. Analytical Moments of the Density Distribution for the Growth Problem

Case	τG_0	m_0	m_1	m_2
3a	1×10^{-1}	1	2.1	6.42
3b	$1\times10^{+1}$	1	12	246
3c	$1\times10^{+3}$	1	1,002	2,004,006

Table 10. Domain Truncation and Partition Parameters Used in the Growth Problem

Case	v^0_{max}	M^0_2	v_{max}	M_2	v_1	N
3a	1×10^0	0.9893	1.369×10^1	0.9993	0.1	20
3b	1×10^2	0.9972	1.140×10^2	0.9991	0.4	25
3c	1×10^4	0.9972	1.144×10^4	0.9991	0.5	30

Evaluations of these moments are tabulated for each of the τG_0 listed in Table 9.

Domain truncation was performed as previously described for aggregation/growth dominant problems. Truncation points, corresponding M_2 values and the parameters of the refined geometrical progression are recorded in Table 10.

The successive substitution strategy (Eq. 47) was used to solve both collocation and Galerkin formulations of this problem. It was found that the collocation formulation resulted in ill-conditioned global matrices. The magnitudes of the derivatives of the interpolation functions increase very rapidly as the element lengths become small. Partitioning the domain according to the GP (Eq. 12) results in a global matrix with entries in the top left corner that are large enough to cause matrix ill-conditioning. The resulting poor solution for case 3a is shown in Figure 4.

A much better conditioned system is obtained if the Galerkin formulation of the problem is used in all elements where

$$\text{element length} < 10\tau G_{max}(v) \tag{81}$$

$G_{max}(v)$ is the maximum value attained by the growth function within the element. The solution of the mixed collocation-Galerkin formulation of the growth problem is shown in Figure 5. Solid lines represent the analytical solution (Eq. 76)

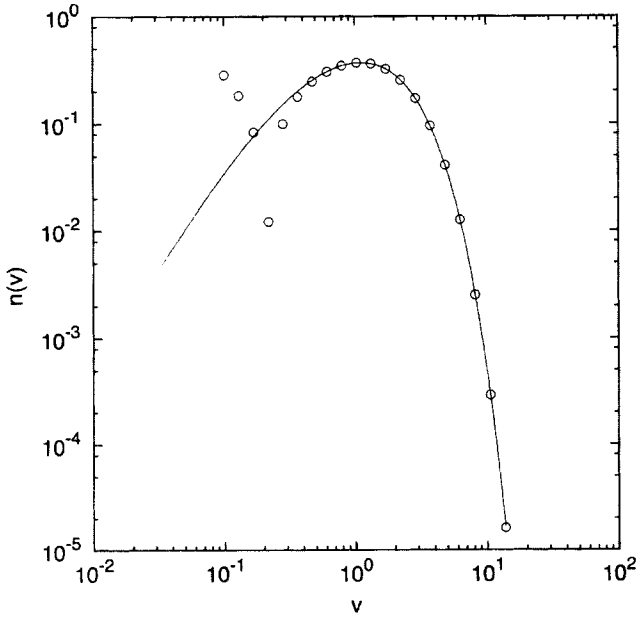

Figure 4. Poor solution of the collocation formulation resulting from matrix ill-conditioning in case 3a.

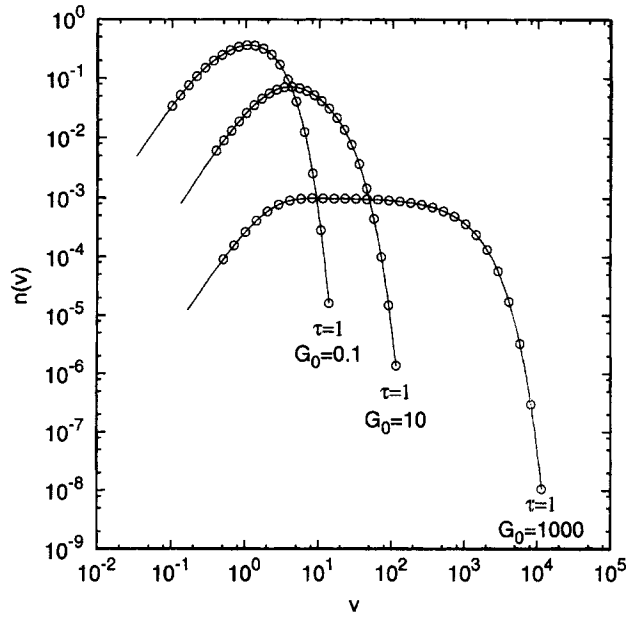

Figure 5. Much improved solutions resulting from mixed collocation-Galerkin formulation of the growth problem.

while the symbols are the nodal values of the finite-element solution for the first and last node of each element.

The errors in the moments of the solution, the mean relative error in the number of particles predicted in an interval, the number of equations to be solved, the CPU requirements, and the number of iterations required for convergence were recorded in Table 11.

Case 4: Combined Aggregation, Growth and Nucleation. The PBE for combined aggregation, growth and nucleation was obtained by setting the breakage function and specific rate of breakage to zero

$$\rho(v,w) = 0 \quad \forall\, v,w \tag{82}$$

$$S(v) = 0 \quad \forall\, v \tag{83}$$

Consider a feed distribution consisting of nuclei of zero size

$$n_{in}(v) = 0 \quad \forall v \epsilon (0,\infty) \tag{84}$$

Additionally, if the aggregation kernel and growth function are both taken to be constant

$$\beta(v,w) = \beta_0 \tag{85}$$

$$G(v) = G_0 \tag{86}$$

Table 11. Errors in Moments and Mean Square Relative Errors of Finite-Element Solution to the Growth Problem

Case	Em_0	Em_1	Em_2	1/N SSRE	N	CPU	N_{it}
3a	0.001%	0.013%	0.064%	1.527×10^{-5}	10	$<1u$	1
3b	0.006%	0.008%	0.080%	5.241×10^{-6}	15	$<1u$	1
3c	0.015%	0.003%	0.067%	8.688×10^{-9}	20	$<1u$	1

Table 12. Analytical Moments of the Density Distribution for Combined Aggregation and Growth Problem

Case	β_0	G_0	m_0	m_1	m_2
4a	1×10^{0}	1×10^{0}	7.321×10^{-1}	7.321×10^{-1}	2.000×10^{0}
4b	1×10^{1}	1×10^{1}	1.318×10^{0}	1.318×10^{1}	2.000×10^{3}
4c	1×10^{2}	1×10^{2}	1.407×10^{0}	1.404×10^{2}	2.000×10^{6}

then the analytical solution to the resulting PBE has been derived by Liao and Hulburt (1976)

$$n(\upsilon) = 2n_0 \exp(-p\upsilon)\frac{I_1(x)}{x} \tag{87}$$

where

$$p = \sqrt{1+\frac{1}{2\beta_0 n_0 G_0 \tau^2}} \tag{88}$$

$$x = \frac{\upsilon}{G_0}\sqrt{2\beta_0 n_0 G_0} \tag{89}$$

and

$$n(0) = n_0 \tag{90}$$

is the number density of nuclei in the product stream.

The constants τ and n_0 were set to unity and three simulations were performed with the β_0 and G_0 values listed in Table 12.

If the PBE is multiplied by υ^i and integrated over the domain $(0,\infty]$ then the following analytical expressions can be derived for the moments of the density distribution:

$$m_0 = \frac{-1+\sqrt{1+2\beta_0 n_0 G_0 \tau^2}}{\beta_0 \tau} \tag{91}$$

$$m_1 = \tau G_0 m_0 \tag{92}$$

$$m_2 = \tau(\beta_0 m_1^2 + 2G_0 m_1) \tag{93}$$

Numerical values of these moments are tabulated to Table 13 below for each of the problems investigated.

Truncation and refinement of the partition were performed as previously described for aggregation/growth dominant problems. The truncation points and the parameters of the refined geometric progression are listed in Table 13.

The mixed collocation-Galerkin formulation of the problem was solved using the successive substitution scheme (Eq. 47). A log-log plot of the finite-element solution to the problem is shown in Figure 6. Solid lines are the analytical solution (Eq. 87) and the symbols are nodal values of the finite-element solution for the first and last node of each element.

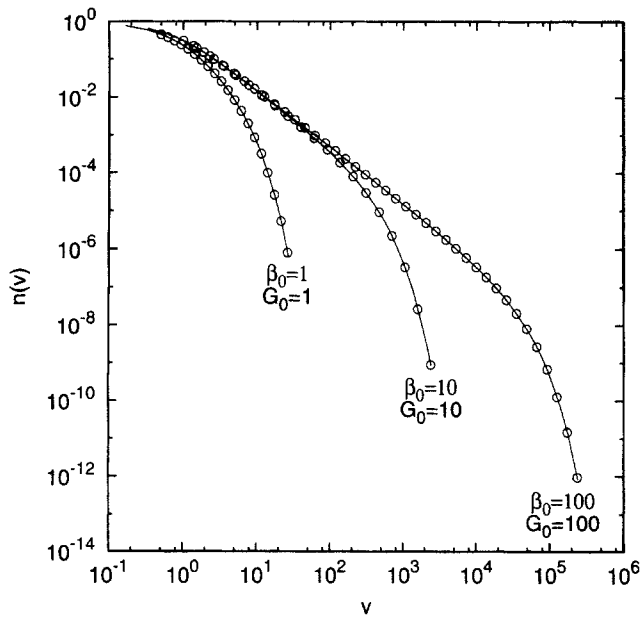

Figure 6. FEM predictions of number density function ($n(v)$) for aggregation and growth problem.

Errors in the moments of the finite-element solution, mean-square relative errors in the number of particles predicted in an interval, the number of equations to be solved, CPU requirements to solve the system, and the number of iterations required for convergence are in Table 14.

Discussion

The case studies of the previous section were selected to be very demanding tests on the finite-element method's convergence capabilities and ability to predict the density distribution and moments correctly. Time constants, growth rates, and so on were chosen so that density distribution of the output stream would be vastly different from that of the feed stream which was used to initialize the iterative procedure (Eqs. 46 and 47). Large changes of the feed distributions were quantified in the first two case studies by the indices of aggregation and breakage. In case 1c (see Table 1) an index of aggregation of 0.999 was achieved. This is indicative of a thousandfold reduction of the number of particles in the feed stream. A similarly large change can be observed for breakage in case 2c (see Table 6), while in the growth example a millionfold increase in the volume of particles of the feed stream was achieved (see Table 6).

Table 13. Domain Truncation and Partition Parameters Used in Combined Aggregation and Growth Problem

Case	$\upsilon^0_{\max}$	M_2^0	$\upsilon_{\max}$	M_2	υ_1	N
4a	2.500×10^{3}	0.9938	2.636×10^{1}	0.9991	0.5	20
4b	2.500×10^{5}	0.9858	2.379×10^{3}	0.9992	1.0	20
4c	2.500×10^{7}	0.9859	2.365×10^{5}	0.9992	1.0	40

Table 14. Errors in Moments and Mean Square Relative Errors of the Finite-Element Solution to the Aggregation and Growth Problem

Case	Em_0	Em_1	Em_2	$1/N$ SSRE	N_{eq}	CPU	N_{it}
4a	0.055%	0.046%	0.013%	7.568×10^{-7}	61	$<1u$	21
4b	0.217%	0.131%	0.141%	5.478×10^{-5}	61	$4u$	240
4c	0.203%	0.135%	0.200%	1.709×10^{-5}	121	$143u$	2,253

To predict the second moment of the density distribution accurately, a method must be capable of solving for a function with values that can change over many orders of magnitude. For instance, the density distribution of case 1c assumes values between 0.286×10^{-18} and 0.500×10^{-3} over the domain of interest. In all cases the finite-element method proved capable of this task. Figures 1, 3, 5 and 6 show excellent agreement between the finite-element solution and the analytical solutions of the problems under study. This excellent agreement is quantified by the low $1/N$ SSRE values listed in Tables 3, 8, 11 and 14. Second moments were also predicted to within one third of a percent of their analytical values.

Accurate prediction of moments requires appropriately chosen domain truncation points. Visual inspection of the $v^2n_h(v)$ curve can be used to satisfy criterion 11 to within $\pm0.1\%$. If additional accuracy is required, the extrapolation procedure described earlier in this article can be used to eliminate much of the time-consuming guesswork associated with finding the upper limit by trial and error.

In a direct comparison with the DPB it was shown that the finite-element method was capable of more accurate predictions of the density distribution. In Figure 2 it can be seen that the SRE values for the FEM are several orders of magnitude smaller than those of the DPB for case 1b. This fact is quantified by a comparison of the $1/N$ SSRE values in Tables 3 and 5. The $1/N$ SSRE values are typically two to three orders of magnitude smaller for the finite-element method.

The DPB algorithm is derived such that the zeroth and first moments of the density distribution are predicted correctly. In Table 5 it can be seen that the first moment is predicted exactly by the DPB. In all cases the finite-element method predicted moments to within 0.2% of their analytical value and made slightly better predictions of the zeroth and second moments than the DPB. Comparable accuracy in predictions of these moments is achieved by the DPB, despite much larger SRE values, due to error cancellations.

Considerably less computational power was used by the finite-element method in obtaining its results. Tables 3 and 5 reveal that the finite-element method converged using 1.85%, 13.6%, and 78.4% of the computational power required by the DPB.

It should also be noted that the finite-element method was initialized using the feed distribution, which in many cases differed from the final converged solution by over ten orders of magnitude. The DPB algorithm would not converge from such poor initial guesses and was initialized from much better starting points that were within an order of magnitude of the final solution. In most practical applications such a good initial guess would not be available.

Figure 2 also highlights one of the shortcomings of the DPB. This method does not span the subdomain $(0, v_1)$. Thus, finite domain error is also incurred at the lower end of the volume domain. A small value of v_1 must be selected to reduce this finite domain error to an acceptably small value. Consequently, the geometric progression requires many elements to span the lower volume range where the solution is changing very little across each element.

Memory requirements of the finite-element method were significantly lower than those of the DPB for two reasons: (i) the FEM is a higher-order method and, hence, is capable of achieving better accuracy than the DPB using fewer parameters (compare N_{eq} values of Tables 3 and 5); (ii) the successive substitution strategy retains the data in diagonal block form. A system of N_{eq} equations will result in a matrix of $(N_{eq}-1)/(p-1)$ overlapping $p\times p$ blocks, where $p-1$ is the order of the interpolation polynomial. The DPB uses a Newton's method which requires an $N_{eq}\times N_{eq}$ Jacobian matrix. For instance, in case 1c the finite-element algorithm solves a system of equations with a matrix consisting of 45 4×4 blocks resulting in 719 nonzero matrix entries whereas the DPB solved a system of equations with a completely dense $781\times781=609961$ nonzero entries.

Conclusions

The following general conclusions can be made with regards to the finite-element method developed in this article:

- The finite-element method proved capable of accurately predicting the solution of the PBE and the moments of its solutions.
- Accurate prediction of the moments of the density distribution requires careful selection of the location of the upper limit of the domain.
- A mixed collocation-Galerkin formulation can be used to avoid the ill-conditioned matrices associated with growth problems.
- The derived method is amenable to error analysis and adaptive mesh refinement technique (see Nicmanis and Hounslow, 1998a,b) which yield further increases in accuracy and computational efficiency.

The finite-element method was found to have the following advantages over the DPB of Litster et al. (1995):

- Using smaller systems of equations to represent the PBE, the finite-element method was found capable of making better predictions of the density distribution.
- The finite-element method was found to be more robust and easier to converge and did not require any problem-specific scaling parameters.
- The finite-element method does not incur any truncation errors at the lower volume range.
- No restrictions are placed on the location of grid points when using the finite-element method. Hence, this method is amenable to adaptive mesh grading techniques whereas the grid of the DPB must be partitioned according to a geometrical progression GP.
- The finite-element solution of the PBE can be a piecewise polynomial of any order, whereas that of the DPB is assumed to be constant within each partition.
- The finite-element method uses significantly smaller amounts of memory when solving the PBE.
- The finite-element method requires significantly smaller amounts of CPU time to converge to a solution.

The finite-element method of this article has the following advantages over the finite methods of other researchers:

- The work of this article is the first method derived to be capable of modeling the full range of particulate behavior, that is, aggregation, breakage, nucleation, and growth.
- The method presented in this article does not require any problem-specific domain scaling.

• The mixed collocation-Galerkin formulation derived in this article can be used to avoid ill-conditioned matrices that would be encountered when using other methods.

• The method of selecting the upper limit of the finite domain can be used to reduce finite domain errors to negligibly small values and to improve estimates of the moments of the density distribution.

Acknowledgments

The authors are indebted to the ORS Committee, Cambridge Commonwealth Trust, and the Dept. of Chemical Engineering at the Univ. of Cambridge for the support that made this work possible.

Notation

$d^b(v)$ = death rate due to breakage
G_0 = growth constant
m_i = i^{th} moment of the density distribution
n_0 = number of nuclei
N_0 = number of nuclei present in the exponential feed distribution
$n_h(v)$ = finite-element solution of the PBE
n_j^e = jth nodal value of element e
N_{eq} = number of equations comprising the system
N_{it} = number of iterations required for the system to converge
v_1 = length of the first element in the GP of the FEM
v_a^e = volume coordinate of the lower limit of element e
v_0 = mean size of the nuclei in the exponential feed distribution

Greek letters

β_0 = size-independent aggregation kernel

Superscripts

a = denotes aggregation
b = denotes breakage
s = the sth iteration

Subscript

in = pertaining to the feed stream

Literature Cited

Batterham, R. J., J. S. Hall, and G. Barton, "Pelletizing Kinetics and Simulation of Full-Scale Balling Circuits," *Proc. 3rd Int. Symp. on Agglomeration*, Nurnberg, West Germany, A136 (1981).

Eyre, D., C. J. Wright, and G. Reuter, "Spline-Collocation with Adaptive Mesh Grading for Solving the Stochastic Collection Equation," *J. Comp. Phys.*, **78**, 288 (1988).

Gelbard, F., and J. H. Seinfeld, "Numerical Solution of the Dynamic Equation for Particulate Systems," *J. Comp. Phys.*, **28**, 357 (1978).

Hill, P. J., and K. M. Ng, "New Discretization Procedure for the Breakage Equation," *AIChE J.*, **41**(5), 1204 (1995).

Hounslow, M. J., "A Discretized Population Balance for Continuous Systems at Steady State," *AIChE J.*, **36**(1), 106 (1990).

Hounslow, M. J., "Asymptotic Particle Size Distributions for Size Independent Aggregation and Growth in a CST," in press (1998).

Hounslow, M. J., R. L. Ryall, and V. R. Marshall, "A Discretized Population Balance for Nucleation, Growth and Aggregation," *AIChE J.*, **34**(11), 1821 (1988).

Hulburt, H. M., and S. Katz, "Some Problems in Particle Technology. A Statistical Mechanical Formulation," *Chem. Eng. Sci.*, **19**, 555 (1964).

Liao, P. F., and H. M. Hulburt, "Agglomeration Processes in Suspension Crystallization," AIChE Meeting, Chicago (Dec. 1976).

Litster, J. D., D. J. Smit, and M. J. Hounslow, "Adjustable Discretized Population Balance for Growth and Aggregation," *AIChE J.*, **41**(3), 1 (1995).

McGrady, E. D., and R. M. Ziff, "Analytical Solutions to Fragmentation Equations with Flow," *AIChE J.*, **34**(12), 2073 (1988).

Marchal, P., R. David, J. P. Klein, and J. Villermaux, "Crystallization and Precipitation Engineering. I: An Efficient Method for Solving Population Balance in Crystallization with Agglomeration," *Chem. Eng. Sci.*, **43**(1), 59 (1988).

Nicmanis, M., and M. J. Hounslow, "An *a posteriori* Error Estimate for the Steady State Population Balance Equation," *Int. J. of Numer. Methods in Eng.*, in press (1998a).

Nicmanis, M., and M. J. Hounslow, "Adaptive Mesh Refinement for the Steady State Population Balance Equation," *Computers Chem. Eng.*, in press (1998b).

Prasher, C. L., *Crushing and Grinding Process Handbook*, Wiley, New York (1987).

Press, W. H., S. A. Teukolsky, W. T. Vetterling, and B. P. Flannery, *Numerical Recipes in Fortran*, 2nd ed., Cambridge University Press, Cambridge, U.K. (1992).

Ramkrishna, D., "Status of Population Balances," *Rev. Chem. Eng.*, **3**, 49 (1985).

Randolph, A. D., and M. A. Larson, *Theory of Particulate Processes*, 2nd ed., Academic Press, New York (1988).

Smit, D. J., "Simulation and Inverse Problems in Aggregation," PhD Thesis, Dept. of Chemical Engineering, University of Cambridge, Cambridge, U.K. (1995).

Smit, D. J., M. J. Hounslow, and W. R. Paterson, "Aggregation and Gelation 1: Analytical Solutions for CST and Batch Operation," *Chem. Eng. Sci.*, **49**(7), 1025 (1993).

Viljoen, H. J., D. Eyre, and C. J. Wright, "Solving Dynamic Equations for the Collection and Evaporation of an Aerosol," *Can. J. Ch. E.*, **68**, 938 (1990).

Wynn, E. J., "Improved Accuracy and Convergence of Discretized Population Balance of Litster et al." *AIChE J.*, **42**(7), 2084 (1996).

Zienkiewicz, O. C., and R. L. Taylor, *The Finite Element Method: Basic Formulation and Linear Problems*, 4th ed., McGraw Hill, U.K., (1989).

Appendix A: Truncation of the Infinite Domain to a Finite Upper Limit

Aggregation/growth dominant problems

If the second moment of the solution of a problem is greater than the second moment of the feed distribution, the problem will be classified as an aggregation/growth dominant problem. In such problems the value of $v_{\max}$ required to satisfy criterion 11 can be several orders of magnitude greater than $v_{\max}^{\text{in}}$: the upper limit of a domain is such that $M_2^{\text{in}} \approx 0.999$. Selection of an appropriate value of $v_{\max}$ is performed as:

(1) Obtain an order of magnitude estimate of the upper limit ($v_{\max}^0$): Simulations are performed and plots of the $v^2 n(v)$ curve are visually inspected. Increasing values of the upper limit of the domain are used until the tail region (region where the curve begins to asymptote towards zero for increasing particle sizes) of this curve is located. An order of magnitude estimate is then located on the tail region. $v_{\max}$ is assumed slightly underestimated: $M_2 < 0.999$.

(2) Refine the partition: The partition is refined (see the next section) to ensure that the finite-element solution is a reasonable approximation of the density distribution $n(v)$ over the truncated domain.

(3) Extrapolate an exponential function through the last element: An exponential function ($\exp(a + bv)$) is extrapolated through the first and last nodes of the last element. The constants (a and b) are determined such that this exponential passes through the points $(v_a, v_a^2 n(v_a))$ and $(v_b, v_b^2 n(v_b))$, where the subscripts a and b denote the first and last nodes of the last element.

(4) M_2 is approximated as follows

$$M_2 \approx \frac{A_1 + A_2}{A_1 + A_2 + A_3} \tag{A1}$$

where the quantities A_1, A_2 and A_3 are defined as follows

$$\begin{aligned} A_1 &:= \int_0^{v_{\max}^0} v^2 n(v)dv \\ &\approx \int_0^{v_{\max}^0} v^2 n_h(v)dv \end{aligned} \tag{A2}$$

$$\begin{aligned} A_2 &:= \int_{v_{\max}^0}^{v_{\max}^f} v^2 n(v)dv \\ &\approx \int_{v_{\max}^0}^{v_{\max}^f} \exp(a + bv)dv \\ &= \frac{\exp(a + bv_{\max}^f) - \exp(a + bv_{\max}^0)}{b} \end{aligned} \tag{A3}$$

$$\begin{aligned} A_3 &:= \int_{v_{\max}^f}^{\infty} v^2 n(v)dv \\ &\approx \int_{v_{\max}^f}^{\infty} \exp(a + bv)dv \\ &= -\frac{\exp(a + bv_{\max}^f)}{b} \end{aligned} \tag{A4}$$

(5) Solve for an improved estimate of $v_{\max}^f$: The expression

$$\frac{A_1 + A_2}{A_1 + A_2 + A_3} = 0.999 \tag{A5}$$

is solved for $v_{\max}^f$ which will be an improved estimate of an upper limit that will satisfy criterion 11. In expression A2 $n_h(v)$ denotes the finite-element solution of the problem. This function is defined later by Eq. 13.

Breakage dominant problems

In breakage dominant problems the second moment of the solution is smaller than the second moment of the feed distribution. Two different points must be located if the solution and its second moment are to be evaluated accurately. The first point $v_{\max_1}$ is the volume coordinate such that criterion 11 can be satisfied. In these problems $v_{\max}^{\text{in}}$ is a reasonable first estimate of $v_{\max_1}$. An improved estimate of $v_{\max_1}$ is obtained using the following procedure:

(1) $v_{\max}^{\text{in}}$ is used as a first estimate of the upper limit to the truncated domain.

(2) The quantities M_2^j are defined as follows

$$M_2^j := \frac{A_1 + A_2 + \ldots + A_j}{\sum_{i=1}^{N} A_i} \tag{A6}$$

where

$$A_i := \int_{v_a^i}^{v_b^i} v^2 n_h^i(v)dv \tag{A7}$$

and N is the total number of elements spanning the domain, $n_h^i(v)$ is the finite-element solution in element i and v_b^i and v_a^i are the upper and lower limits of element i respectively.

(3) M_2^js are evaluated for increasing values of j until

$$M_2^j > 0.999 \tag{A8}$$

(4) Then we set

$$v_{\max_1} = v_b^j \tag{A9}$$

If the birth rate due to breakage is to be calculated to high accuracy at $v = v_{\max_1}$, then further extension of the domain is necessary. A second point $v_{\max_2}$ is identified such that a second criterion may be satisfied

$$\frac{\int_{v_{\max_1}}^{v_{\max_2}} \rho(v,w)S(w)n(w)dw}{\int_{v_{\max_1}}^{\infty} \rho(v,w)S(w)n(w)dw} > 0.999 \tag{A10}$$

Using this criterion, the point $v_{\max_2}$ may be found such that truncation errors in the birth rate due to breakage are negligibly small for all volume coordinates in the domain $v \in (0, v_{\max_1})$. The point $v_{\max_2}$ is located as follows:

(1) An exponential function ($\exp(a + bv)$) is extrapolated through the element containing $v_{\max_1}$. The constants (a and b) are determined such that this function passes through the points (v_a, p_a) and $(v_{\max_1}, p_b)$ where

$$p_a = \rho(v_{\max_1}, v_a)S(v_a)n(v_a)$$

$$p_b = \rho(v_{\max_1}, v_{\max_1})S(v_{\max_1})n(v_{\max_1})$$

and v_a is the lower limit of the element containing $v_{\max_1}$.

(2) The lefthand side of criterion 103 is approximated as follows

$$\frac{\int_{v_{\max_1}}^{v_{\max_2}} \rho(v,w)S(w)n(w)dw}{\int_{v_{\max_1}}^{\infty} \rho(v,w)S(w)n(w)dw} \approx \frac{A_1}{A_1 + A_2} \tag{A11}$$

where

$$\begin{aligned} A_1 &:= \int_{v_{\max_1}}^{v_{\max_2}} \exp(a + bv)dv \\ &= \frac{\exp(a + bv_{\max_2}) - \exp(a + bv_{\max_1})}{b} \end{aligned} \tag{A12}$$

$$\begin{aligned} A_2 &:= \int_{v_{\max_2}}^{\infty} \exp(a + bv)dv \\ &= \frac{\exp(a + bv_{\max_2})}{b} \end{aligned} \tag{A13}$$

(3) The expression

$$\frac{A_1}{A_1 + A_2} = 0.999 \tag{A14}$$

is solved for v_{max_2}.

A solution is found over the interval (v_{max_1}, v_{max_2}) so that a better estimate of the birth rate due to breakage may be obtained in the interval $(0, v_{max_1})$. When calculating moments, the solution is only considered within the interval $(0, v_{max_1})$.

Appendix B: Analytical Solution of the Steady-State Breakage Equation

Using the breakage function and specific rate of breakage selected for case 2, the PBE for breakage alone becomes

$$\frac{n(v) + n_{in}(v)}{\tau} = 2\int_v^\infty n(w)dw - vn(v) \tag{B1}$$

where $n_{in}(v)$ is the exponential feed distribution (Eq. 51).

If the above PBE is multiplied by τ and differentiated with respect to v, the following first-order ODE may be obtained

$$\frac{dn(v)}{dv} + \frac{3\tau}{1+\tau v} n(v) = \frac{1}{1+\tau v} \frac{dn_{in}(v)}{dv} \tag{B2}$$

By considering the breakage PBE (Eq. B1) at the point $v = 0$, we obtain the appropriate boundary condition

$$\begin{aligned} n_0 &= 2\tau m_0 + n_{in}(0) \\ &= 2\tau m_0 + \frac{N_0}{v_0} \end{aligned} \tag{B3}$$

An expression for the zeroth moment is obtained by integrating Eq. B1 from zero to infinity

$$\begin{aligned} m_0 &= \tau m_1 + m_0^{in} \\ &= \tau m_1^{in} + m_0^{in} \end{aligned} \tag{B4}$$

The second equality holds true since volume is conserved in a breakage only problem.

Expressions for m_0^{in} and m_1^{in} may be readily obtained by integration of the exponential feed distribution

$$\begin{aligned} m_0^{in} &= \int_0^\infty n_{in}(v)dv \\ &= \int_0^\infty \frac{N_0}{v_0} \exp(-v/v_0)dv = N_0 \end{aligned} \tag{B5}$$

$$\begin{aligned} m_1^{in} &= \int_0^\infty v n_{in}(v)dv \\ &= \int_0^\infty \frac{N_0}{v_0} v \exp(-v/v_0)dv \\ &= N_0 v_0 \end{aligned} \tag{B6}$$

Expressions B3, B4, B5, and B6 are combined to obtain the, boundary condition in terms of the problem parameters

$$n_0 = 2\tau N_0(\tau v_0 + 1) + \frac{N_0}{v_0} \tag{B7}$$

The integrating factor $I(v)$ is evaluated as

$$I(v) = \exp\left(\int_0^v \frac{3\tau}{1+\tau w} dw\right) = (1+\tau v)^3 \tag{B8}$$

The solution to the ODE B2 with the boundary condition B7 is

$$n(v) = \frac{n_0}{I(v)} + \frac{1}{I(v)} \int_0^v \frac{I(t)}{1+\tau t} \frac{dn_{in}(t)}{dv} dt \tag{B9}$$

Integration and algebraic manipulation of this expression yields the solution to the breakage PBE B1

$$n(v) = \frac{N_0\left[(1+\tau v)^2 + 2\tau v_0(1+\tau[v_0+v])\right]}{v_0(1+\tau v)^3 \exp\left(\frac{v}{v_0}\right)} \tag{B10}$$

Manuscript received Sept. 15, 1997, and revision received Mar. 4, 1998.